
Active Sway Control of a Gantry Crane by an Electrical Ducted Fan

Mohammad Javad Maghsoudi and Z. Mohamed

Faculty of Electrical Engineering, Universiti Teknologi Malaysia, 81310 UTM Johor Bahru, Johor, Malaysia

(Received 4 June 2013; accepted 23 May 2014)

Sway reduction is very vital in a nonlinear oscillatory system such as a gantry crane. In this paper, a new design is proposed for active sway control of a gantry crane using an electrical ducted fan. The thrust force developed by the motor is used to cancel out payload oscillation. A dynamic model of the crane with a ducted fan is derived and simulated using Matlab. Performance of the proposed technique is investigated for a crane subjected to initial sway and an external force input. In addition, cases with different payloads and cable lengths are also studied. Simulation results show satisfactory performance of the fan-controlled system in eliminating the payload sway. The proposed design can also handle changes in payload and cable length. A main advantage of this approach is that it does not require modeling of the crane in real time experiments.

1. INTRODUCTION

Vibration control is crucial in flexible structures where their movement produces undesired vibration. Although flexible systems are lighter and faster than rigid ones, their motion-induced vibration is a drawback that limits their applications. In order to reduce the system vibration, several control approaches have been proposed by researchers. These include, active control of a grinding machine,¹ adaptive control of a drill string,² active vibration control of a ring-stiffened cylindrical shell³ and active vibration control of smart plates.⁴

Gantry cranes are flexible structures that are commonly used in material handling systems in factories, warehouse, shipping yards, and nuclear facilities where heavy loads must be transferred from a specific place to a desired location. However, the crane movement induces undesirable payload sway.⁵ This undesired load swing negatively influences the productivity and causes a drop in efficiency, load damages, and even accidents. Speed is a focal point in industries as it translates into the productivity and efficiency of the system. However, fast maneuvers tend to excite sway angles of the hoisting line, and this can result in a higher residual sway that degrades the overall performance. At very low speeds, the payload sway is not important and can be ignored. Nevertheless, at a higher speed, these sway angles become larger and significant and cause the payload difficulty in settling down when unloading. The overall system performance will be affected when significant sway angle of the payload occurs during and after the movement of a gantry crane. This is a very severe problem, especially for applications in the industries that require high positioning accuracy, small swing angle, short transportation time, and high safety.⁶

A number of techniques have been proposed for control of gantry cranes. The control objective is to move the trolley to a required position as fast as possible with low payload oscillation. The control algorithms can be categorized into feed-forward and feedback control strategies. The feed-forward control strategy mainly involves command shaping techniques and optimal control. An approach in command shaping techniques known as input shaping has been proposed and has received considerable attention in vibration control.⁷ An input shaping technique for reduction of the residual vibration of a

gantry crane has also been proposed.^{8,9} The closed-loop control algorithms include linear quadratic regulator (LQR) technique, state feedback, and nonlinear control. The LQR technique is utilized to track the reference trajectories,¹⁰ the state feedback control strategy is used to hoist, stabilize, and deliver the payload¹¹ and a nonlinear control scheme incorporating parameter adaptive mechanism is utilized to ensure the overall close-loop system stability⁶ have been proposed by researchers. On the other hand, an acceptable system performance without payload sway that accounts for system changes by developing a hybrid controller consisting of both feed-forward and feedback control techniques has been successfully implemented on a gantry crane.¹²

Although many control strategies have been applied on different type of cranes to reduce the payload sway, no work has been conducted on the direct control of the payload sway. Several researchers have used ducted fans to control the swinging payloads, such as spy cameras¹³ and indoor service robots.¹⁴ In this paper, a new sway control strategy is proposed that utilizes an electrical ducted fan to directly control the payload sway of a gantry crane. The thrust force of an electrical ducted fan, installed on top of the hook, can be used to significantly reduce residual sway. The proposed technique can handle initial sway, external disturbances and changes in payloads and cable lengths.

2. DYNAMIC MODEL OF A GANTRY CRANE

The gantry crane can be considered as a simple cart and pendulum system.¹² Figure 1 shows a schematic diagram of a trolley and payload system considered in this study. M , m , l , b , d , F_e , x , and θ represent trolley mass, payload mass, cable length, coefficient of payload friction, coefficient of trolley friction, external force, trolley displacement, and angular displacement of payload, respectively. Table 1 shows the system parameters used in these investigations.

There are several methods to derive the mathematical equations that represent the trolley and payload system. In this work, Lagrange's equation is used to derive the mathematical expression for the model. The system has two numbers of independent generalized coordinate, namely trolley displacement x and angular displacement of payload oscillation. The

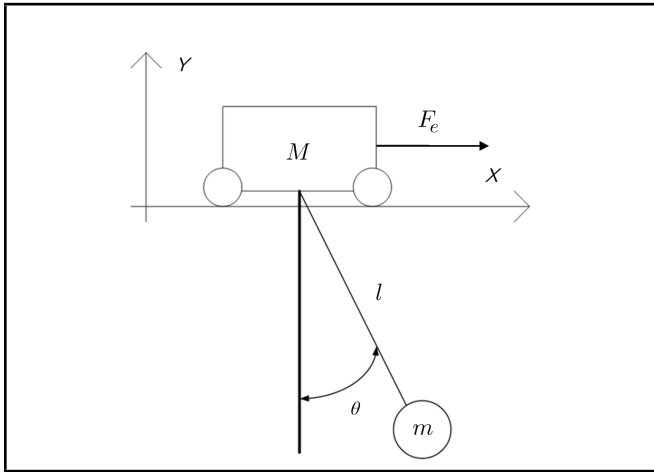


Figure 1. Schematic diagram of a gantry crane.

Table 1. System Parameters.

Variables	Values
mass of trolley, M	1 kg
mass of payload, m	1.1 kg
gravitational constant, g (m)	9.8 m/s ²
trolley friction constant, d	20 Ns/m
constant of payload friction, b	0.001 Ns/m
length of cable, l	0.45 m

standard form for Lagrange's equation is given as

$$\frac{d}{dt} \left[\frac{\partial L}{\partial \dot{q}_i} \right] - \frac{\partial L}{\partial q_i} = Q_i; \quad (1)$$

where L , Q_i and q_i represent Lagrangian function, non-conservative generalized forces, and independent generalized coordinate. The Lagrangian function can be written as:

$$L = T - V; \quad (2)$$

where T and V are kinetic and potential energies, respectively. Therefore, the Lagrangian function can be obtained as:

$$L = \frac{1}{2} (m\dot{x}^2 + M\dot{x}^2 + ml^2\dot{\theta}^2) + m\dot{x}l\cos\theta + mgl\cos\theta. \quad (3)$$

Analyzing Eq. (3) yields:

$$\frac{\partial L}{\partial \dot{x}} = m\dot{x} + M\dot{x} + ml\dot{\theta}\cos\theta; \quad (4)$$

$$\frac{d}{dt} \left[\frac{\partial L}{\partial \dot{x}} \right] = m\ddot{x} + M\ddot{x} - ml\dot{\theta}^2\sin\theta + ml\ddot{\theta}\cos\theta; \quad (5)$$

$$\frac{\partial L}{\partial \dot{\theta}} = ml^2\dot{\theta} + m\dot{x}l\cos\theta; \quad (6)$$

$$\frac{d}{dt} \left[\frac{\partial L}{\partial \dot{\theta}} \right] = ml^2\ddot{\theta} + m\dot{x}l\dot{\theta}\sin\theta + m\ddot{x}l\cos\theta. \quad (7)$$

Utilizing Eqs. (4) to (7) and Eq. (1) yields nonlinear differential equations of the system as:

$$(m + M)\ddot{x} + ml\ddot{\theta}\cos\theta - ml\dot{\theta}^2\sin\theta - \dot{x} = F_e; \quad (8)$$

$$ml^2\ddot{\theta} + ml\dot{x}\cos\theta + mgl\sin\theta + b\dot{\theta} = 0. \quad (9)$$

In Matlab Simulink, the nonlinear equations are modeled as a single input multi output (SIMO) system and the model will be used for controller design and verification.

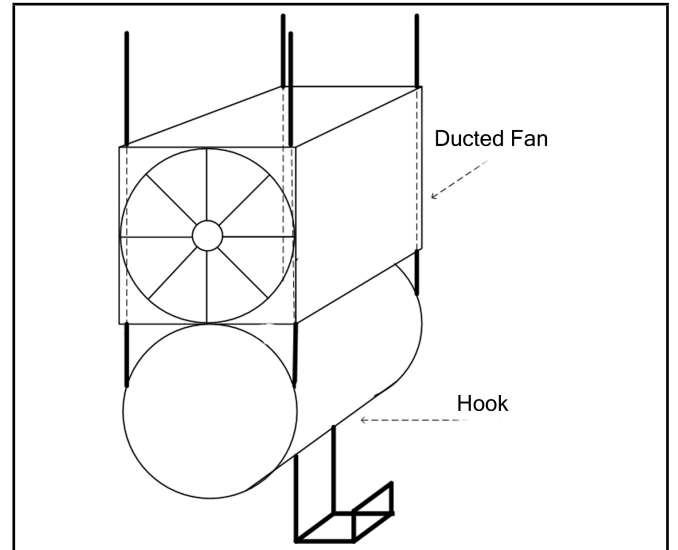


Figure 2. An electrical ducted fan installed on top of the hook.

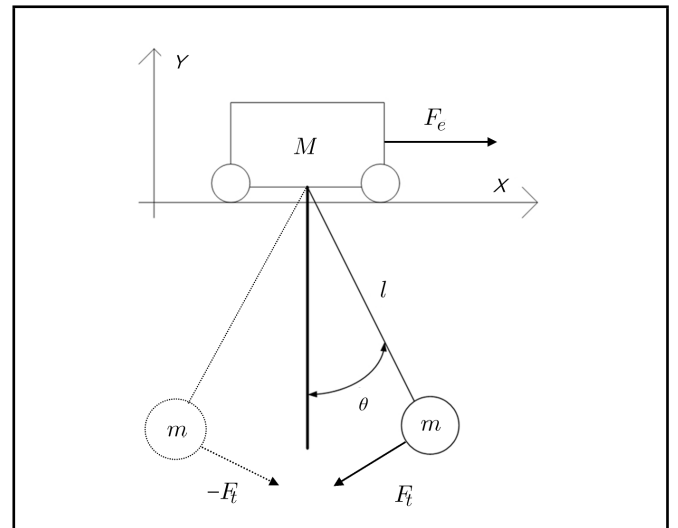


Figure 3. Schematic diagram of the gantry crane with fan.

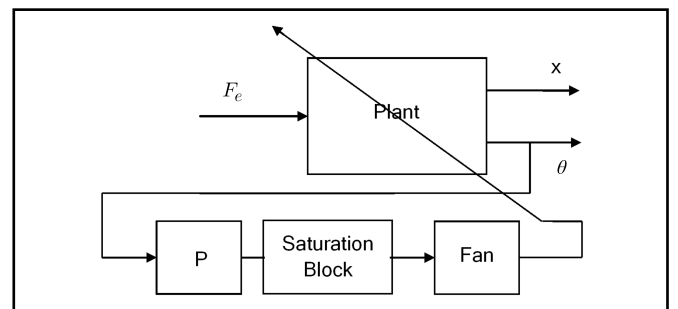


Figure 4. Fan control scheme.

3. FAN CONTROLLED SYSTEM

The gantry crane system is modeled using nonlinear equations as in Eqs. (8) and (9). Although this model is simply utilized for numerical simulation, finding an accurate model that gives similar behavior as the real system is usually very difficult. Model uncertainty can cause serious problems in terms of system performance and stability in real systems. Moreover, applying an external force to a nonlinear gantry crane system produces a considerable amount of sway in the transient and

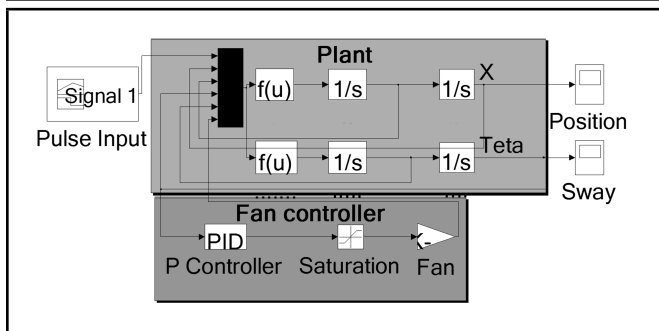


Figure 5. Simulation of the fan control scheme.

steady states of the system. As this payload sway is the most important specification in control objective, having an intelligent payload that can eliminate the sway actively is beneficial.

In this work, a payload equipped with an electrical ducted fan as an active controller is proposed. As shown in Fig. 2, the fan is installed on top of the hook. Most of the industrial gantry cranes are equipped with four strong cables to hoist the load. The fan can be installed in such a way that these cables support the fan and keep the fan parallel to the hook in order to prevent it from undesirable rotation. Moreover, hoisting is considered where the cable length can be reduced or increased to move in vertical directions. For this reason, these cables are designed to pass through four holes in the frame of the fan. The schematic diagram of the system including the fan is shown in Fig. 3. The thrust force (F_t) of the fan is able to move the payload to the left and right intelligently. The payload oscillation can be cancelled by applying the thrust force as in Eq. (10).

$$ml\ddot{\theta} + m\ddot{x} \cos \theta + mg \sin \theta + (b/l)\dot{\theta} = -F_t. \quad (10)$$

It is assumed that F_t acts similar to the air friction force of the payload. The hook and fan are considered as a lumped mass. As shown in Fig. 3, when the payload moves to right side, F_t will react in the opposite direction to cancel the sway. Similarly, when the payload moves to left side, F_t will also react in the opposite direction. This can be done by changing the rotation direction of the fan using its motor driver.

Figure 4 shows the control system of a fan that consists of an encoder to measure the sway angle θ , a proportional controller to command the driver of the fan, a saturator to limit the input of the driver, and a driver to change the direction and voltage level of fan. An AC or DC fan motor compatible with the specific design can be used. The closed-loop controller of the fan tries to keep θ near zero continuously. In other words, any oscillation regardless of its source, whether it is caused by the crane’s movement or by the wind—can be cancelled in the right or left direction. The proposed approach may be feasible using a new carbon made electrical turbo fan weighing 0.12 kg with a diameter of only 0.12 m that can produce thrust of 40 N.¹⁵ It should be mentioned that as the fan controller is independent of the crane controller, other methods, such as input shaping or closed loop controllers, can be used in parallel for the cases where the load is too heavy compared to the fan thrust.

4. SIMULATION RESULTS AND DISCUSSION

In this section, the control scheme is implemented and tested within the simulation environments, and the corresponding re-

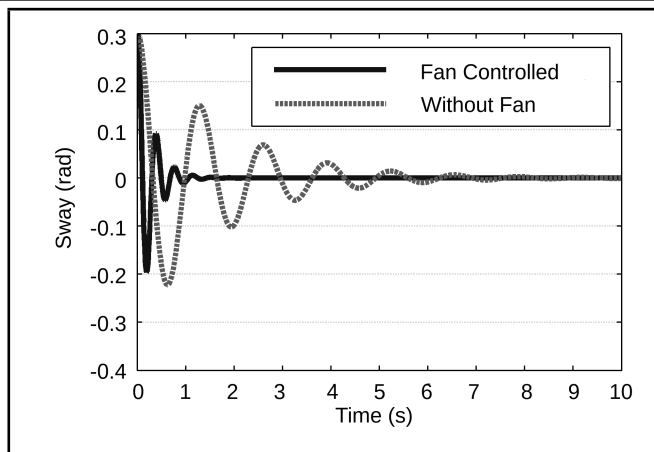


Figure 6. Sway of payload (initial $\theta = 0.3$ rad).

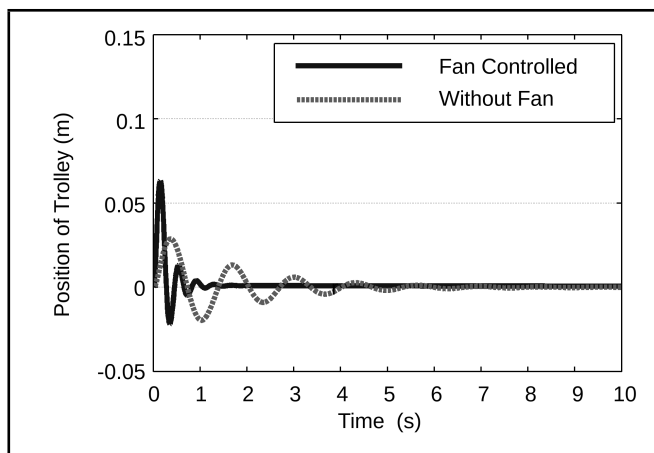


Figure 7. Position response of the trolley (initial $\theta = 0.3$ rad).

sults are presented. A personal computer with Intel Core2 Duo CPU, 2.1 GHz clock frequency and Simulink was utilized for simulation of the controller. Based on the system illustrated in Fig. 5), two functions correspond to position and sway of the model:

$$\ddot{x} = \frac{ml\dot{\theta}^2 \sin \theta + mg \sin \theta \cos \theta - d\dot{x}}{M + m \sin^2 \theta} + \frac{b/l \dot{\theta} \cos \theta + F_t \cos \theta - F_e}{M + m \sin^2 \theta} \quad (11)$$

$$\ddot{\theta} = \frac{-ml\dot{\theta}^2 \sin \theta \cos \theta - (m + M)g \sin \theta + d\dot{x} \cos \theta}{l(M + m \sin^2 \theta)} + \frac{-(1 + M/m)(b/l \dot{\theta} + F_t) + F_e \cos \theta}{l(M + m \sin^2 \theta)} \quad (12)$$

In this experiment, the proportional controller with a gain of 20 is used. The fan is considered as a linear voltage to force convertor with a coefficient of 4. Moreover, maximum and minimum saturation limits are set to +10 volt and -10 volts, respectively.

In the first experiment, the performance of the active sway controller to an initial existing sway was investigated. Thus, a condition with no external input ($F_e = 0$) and initial existing sway ($\theta = 0.3$ rad) was considered. Figures 6 and 7 show simulation results of the payload sway and trolley position response respectively, both without and with a fan-controlled

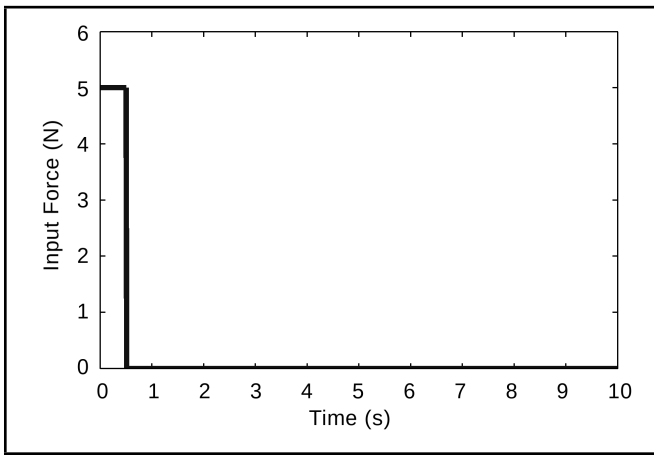


Figure 8. Force Input to the system.

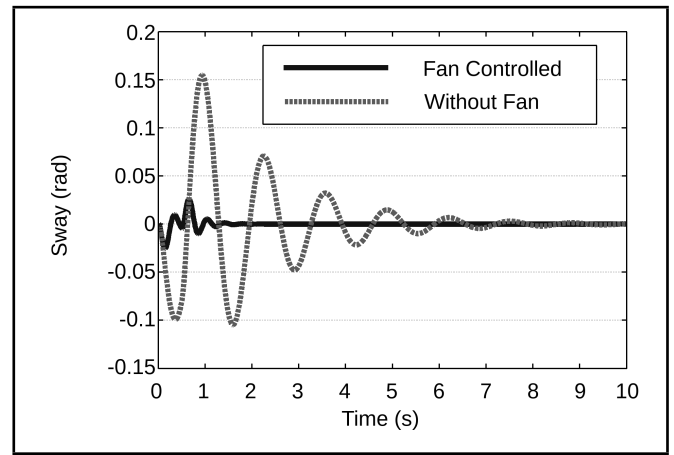


Figure 10. Sway of payload (pulse input).

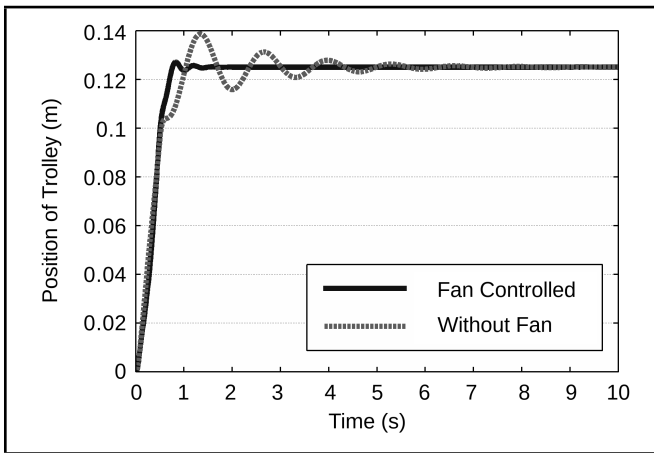


Figure 9. Position response of the trolley (pulse input).

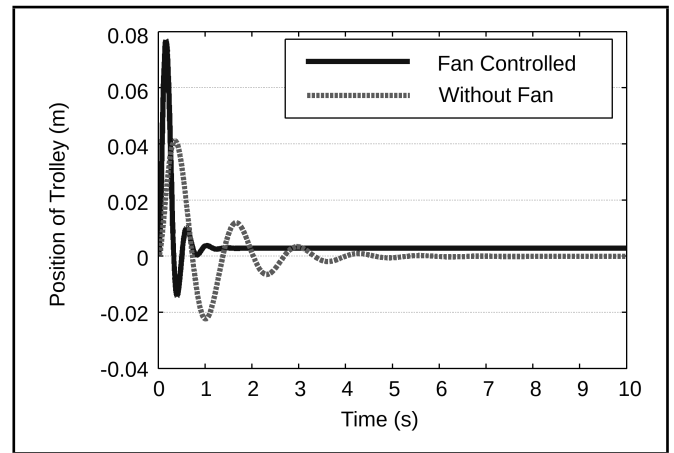


Figure 11. Position response of the trolley (initial $\theta = 0.3$ rad, $m = 1.7$ kg).

system. It was noted that, for payload sway, the thrust force of a fan can eliminate the residual oscillation in a much shorter time (less than two seconds), while without the ducted fan, the system needs more time to eliminate the payload oscillation (about eight seconds). Considering zero sway as the desired response, Integrated Absolute Error (IAE) for a fan-controlled system and a system without a fan were obtained as 6.5463 and 34.3925, respectively. Moreover, because the sway of the payload and the position of the trolley have a direct relationship, the initial payload sway caused the trolley to oscillate. Thus, a reduction of the payload sway is important as it leads to a fast and accurate positioning. It was observed that although a fan-controlled system has a higher initial oscillation compared to the system without a fan, it reaches a steady state faster. In this case, settling times of 0.245 seconds and 0.535 seconds were achieved for the fan-controlled system and the system without a fan, respectively. Moreover, it should be noted that a fan-controlled system needed less than two seconds to reach the steady state, whereas eight seconds is needed for the system without fan.

In the second experiment, the system with an external force and without initial sway was considered. In this case, a pulse input with 5 N force for a duration of 0.5 seconds was used, as shown in Fig. 8. As a result, the crane moves to 0.125 m. As depicted in Fig. 9, the position response of the trolley in fan-controlled system was faster (shorter settling time) with less overshoot. The settling times were obtained as 0.73 seconds and 4.08 seconds with and without a fan, respectively.

Figure 10 shows that the proposed control scheme was able to reduce the payload sway significantly. The IAE values were obtained as 1.1088 and 23.7320 for the system with and without a fan, respectively. Moreover, the proposed control system was able to eliminate the sway within two seconds, whereas the system without a fan needed more than eight seconds to eliminate the sway.

Based on the previous case with $m = 1.1$ kg and $l = 0.45$ m, two cases were studied with $m = 1.7$ kg and $l = 0.45$ m (increased payload) and $m = 1.1$ kg and $l = 0.7$ m (increased cable length). Similarly, a condition with an initial sway of 0.3 rad without external input was considered first. Figures 11 and 12 show the trolley position responses with $m = 1.7$ kg and $l = 0.7$ m, respectively, with and without a fan control. In both cases, faster settling times were achieved with the fan-controlled system. However, a slight steady state error was noted with the system. Table 2 summarizes settling times obtained in all cases. It is noted, that an improvement of almost two-folds was achieved using the fan-controlled system as compared to the system without a fan control.

Figures 13 and 14 show payload sway with $m = 1.7$ kg and $l = 0.7$ m, respectively, for both systems. In both cases, the fan-controlled system was able to reduce the payload sway significantly, within less than two seconds. IAE values for all the cases are summarized in Table 2. It was noted that the sway was reduced almost five times with the fan-controlled system. Similar results obtained with different lengths and payloads demonstrate that the proposed fan-controlled system is able to

Table 2. Settling times and IAE values of system responses (initial $\theta = 0.3$ rad).

System		Settling time (s)		IAE	
m (kg)	l (m)	Normal	Fan-Controlled	Normal	Fan-Controlled
1.1	0.45	0.535	0.245	34.3925	6.5463
1.7	0.45	0.59	0.285	22.4666	5.6147
1.1	0.70	0.725	0.305	51.2193	8.4006

Table 3. Settling times and IAE values of system responses (pulse input).

System		Settling time (s)		IAE	
m (kg)	l (m)	Normal	Fan-Controlled	Normal	Fan-Controlled
1.1	0.45	4.08	0.73	23.7320	1.1088
1.7	0.45	2.845	0.775	15.2906	1.1664
1.1	0.70	5.84	0.915	25.1863	1.1071

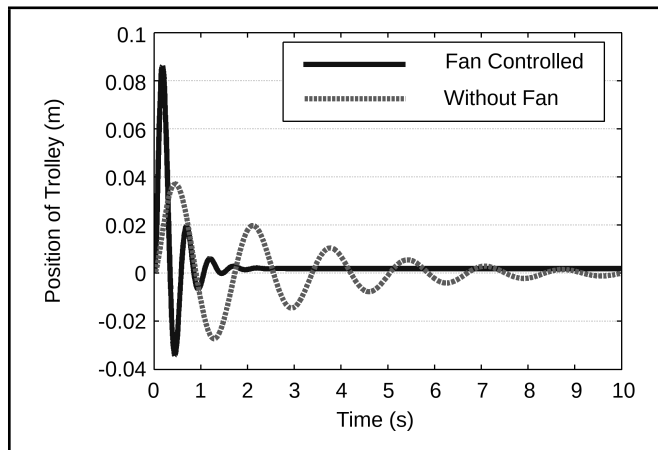


Figure 12. Position response of the trolley (initial $\theta = 0.3$ rad, $l = 0.7$ m).

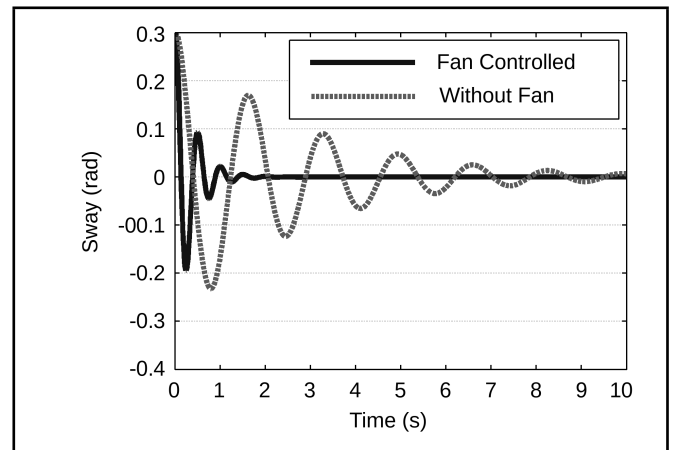


Figure 14. Sway of payload (initial $\theta = 0.3$ rad, $l = 0.7$ m).

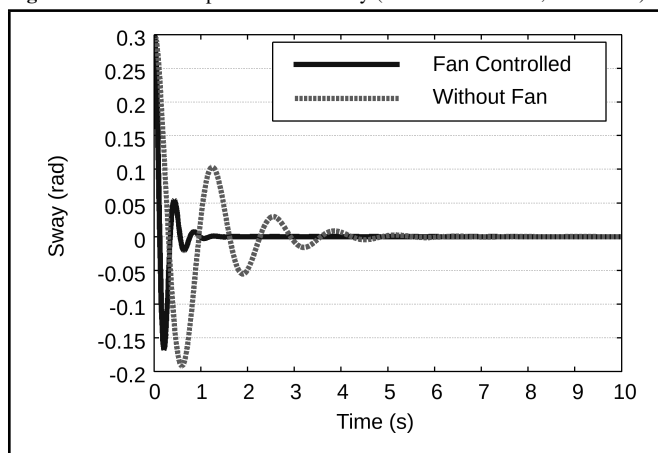


Figure 13. Sway of payload (initial $\theta = 0.3$ rad, $m = 1.7$ kg).

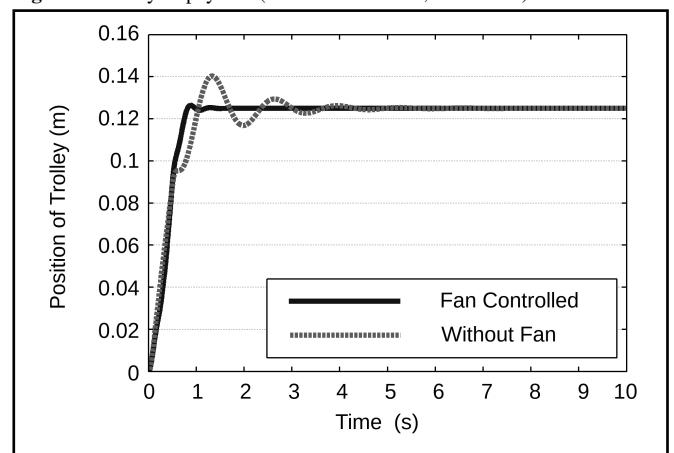


Figure 15. Position response of the trolley (pulse input, $m = 1.7$ kg).

handle changes in the system parameters.

Experiments with a pulse force input, as shown in Fig. 8, were then considered. Figures 15 and 16 show trolley position responses with $m = 1.7$ kg and $l = 0.7$ m, respectively, for both systems. In addition, Figs. 17 and 18 show payload sway for both cases. In both cases, the fan-controlled system showed a similar performance to the first case ($m = 1.1$ kg and $l = 0.45$ m) with faster settling time, less overshoot and less payload sway. Table 3 summarizes settling times and IAE values for the three cases with and without fans. Again, these results demonstrate that the proposed fan-controlled system is able to handle different cable lengths and payloads where similar system performance is achieved.

The results demonstrate that installing an electrical ducted fan on the crane can improve the performance of the system

significantly. One of the most useful advantages of the proposed approach is that it does not need to be modelled after the crane. Therefore, difficulties of modeling for industrial cranes, effects of uncertainties (including changes of load and length during hoisting), and effects of disturbances, such as wind, can be reduced.

5. CONCLUSION

A unique design has been proposed to enable active sway control of a gantry crane by using an electrical ducted fan. The fan is installed in such a way that the thrust force cancels out the oscillation. The proposed design does not need modeling and can overcome parameter uncertainties, such as changes in payload and cable length during hoisting. In addition, the controller is completely independent of the existing gantry crane

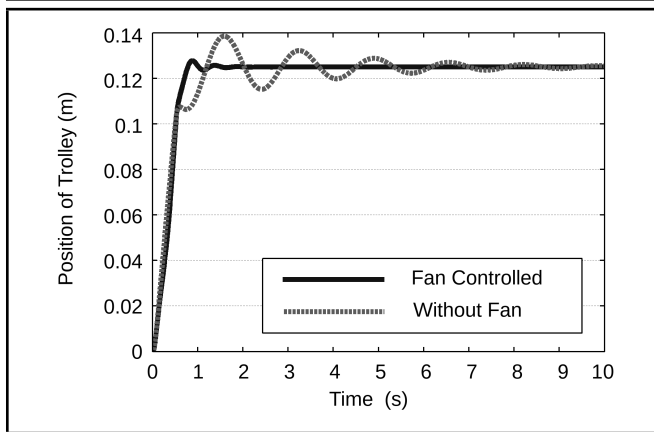


Figure 16. Position response of the trolley (pulse input, $l = 0.7$ m).

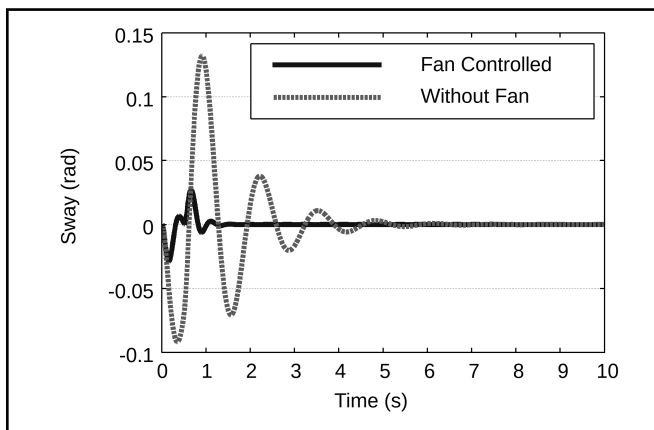


Figure 17. Sway of payload (pulse input, $m = 1.7$ kg).

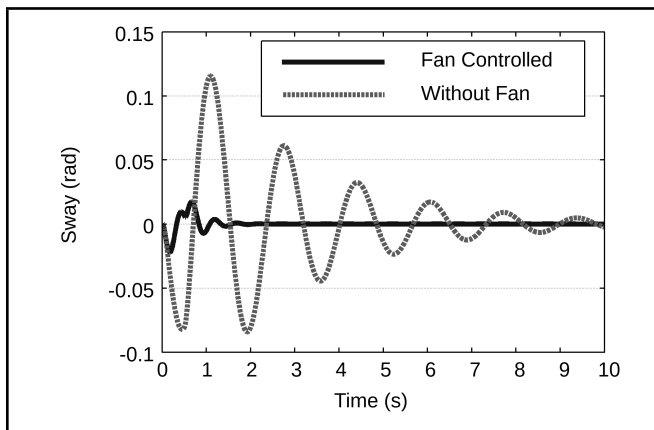


Figure 18. Sway of payload (pulse input, $l = 0.7$ m).

controller. The controller uses a simple proportional controller in a closed loop system. Experiments with several conditions have been simulated in Simulink that have verified acceptable performance of the proposed design in eliminating the existing sway of the gantry crane. The controller has also shown to be able to handle uncertainties in payload and cable length.

REFERENCES

- ¹ Garitaonandia, I., Albizuri, J., Hernandez-Vazquez, J. M., Fernandes, M. H., Olabarrieta, I. and Barrenetxea, D. Redesign of an active system of vibration control in a centerless grinding machine: Numerical simulation and practical implementation, *Precis. Eng.*, **37**(3), 562–71, (2013).
- ² Majeed, F. A., Karki, H., Karkoub, M. and Magid, Y. L. A. Experimental Verification of Drill String Vibration Suppression Using an Adaptive Self-Tuning Controller, *Int. J. Acoust. Vib.*, **18**(1), 20–6, (2013).
- ³ Kwak, M.K. and Yang, D. H. Active vibration control of a ring-stiffened cylindrical shell in contact with unbounded external fluid and subjected to harmonic disturbance by piezoelectric sensor and actuator, *J. Sound. Vib.*, **332**(20), 4775–4797, (2013).
- ⁴ Kapuria, S. and Yasin, M. Y. Active vibration control of smart plates using directional actuation and sensing capability of piezoelectric composites, *Acta Mech.*, **224**(6), 1185–1199, (2013).
- ⁵ Butler, H., Honderd, G. and Van Amerongen, J. Model reference adaptive control of a gantry crane scale model, *IEEE Control Syst. Mag.*, **11**(1), 57–62, (1991).
- ⁶ Yang, J. H. and Yang, K. S. Adaptive coupling control for overhead crane systems, *Mechatronics*, **17**(23), 143–52, (2007).
- ⁷ Mohamed, Z., Martins, J. M., Tokhi, M. O., Sa da Costa, J. and Botto, M. A. Vibration control of a very flexible manipulator system, *Control Eng. Pract.*, **13**(3), 267–277, (2005).
- ⁸ Maghsoudi, M., Mohammed, Z., Pratiwi, A., Ahmad, N. and Husain, A. An experiment for position and sway control of a 3D gantry crane. *4th International Conference on Intelligent and Advanced Systems (ICIAS)*. Kuala Lumpur, Malaysia, 497–502, (2012).
- ⁹ Saeidi, H., Naraghi, M. and Raie, A. A. A neural network self tuner based on input shapers behavior for anti sway system of gantry cranes, *J. Vib. Control*, **19**(13), 1936–1949, (2013).
- ¹⁰ Grassin, N., Retz, T., Caron, B., Bourles, H., and Irving, E. Robust control of a travelling crane. *Proceedings of the European Control Conference Grenoble, France*, 2196–2201, (1991).
- ¹¹ Kim, Y-S., Hong, K-S. and Sul, S-K. Anti-sway control of container cranes: inclinometer, observer, and state feedback, *Int. J. Control Autom.*, **2**(4), 435–449, (2004).
- ¹² Sorensen, K. L, Singhose, W. and Dickerson, S. A controller enabling precise positioning and sway reduction in bridge and gantry cranes, *Control Eng. Pract.*, **15**(7), 825–837, (2007).
- ¹³ McKerrow, P. J. and Ratner, D. The design of a tethered aerial robot. *International Conference on Robotics and Automation*, IEEE, 355–360, (2007).
- ¹⁴ Zelei, A, Kovács, L. L. and Stépán, G. Computed torque control of an under-actuated service robot platform modeled by natural coordinates, *Commun Nonlinear Sci.*, **16**(5), 2205–2217, (2011).
- ¹⁵ Bulk, R. Turbo Fan 4000, Retrieved from <http://www.rbc-kits.com/shop/index.php?a=viewProd&productId=260>, (Accessed June 1, 2013).